J. Fluid Mech. (1986), *vol.* 167, *pp.* 199–217
Printed in Great Britain

Liquid-metal flow in a thin conducting pipe near the end of a region of uniform magnetic field

By JOHN S. WALKER

Department of Theoretical and Applied Mechanics,
University of Illinois, Urbana, IL 61801, U.S.A.

(Received 10 July 1985)

This paper treats the liquid-metal flow in a straight circular pipe with a thin metal wall. A strong magnetic field is applied by a magnet with parallel poles that end abruptly. In the plane midway between the magnet poles: (*a*) far upstream, the flow is uniform, fully developed in a uniform magnetic field; (*b*) as the flow enters the non-uniform magnetic field near the end of the magnet, the flow moves away from the central part of the pipe and becomes concentrated as two jets near the points where the magnetic field is tangential to the pipe wall; (*c*) further downstream where the magnetic field strength is $O(c^{\frac{1}{4}})$ compared with its value upstream, the flow migrates from these jets back towards a uniform flow distributed over the entire pipe cross-section. Here, c is the wall conductance ratio, which is assumed to be small. The analysis also applies to flow into the magnetic field, because inertial effects and induced magnetic fields are neglected. There are circulations of electric current in planes parallel to the magnet poles. These currents produce a pressure drop in addition to that for two fully developed flows in a uniform magnetic field and in no magnetic field, joined at the end of the magnet. This pressure drop is given by $0.9336\,\beta^{\frac{1}{3}}c^{\frac{2}{3}}\sigma\, V_0 B_0^2 L$, where β is a measure of the magnetic field gradient with a minimum value of $2/\pi$, σ is the liquid metal's electrical conductivity, V_0 is the average velocity, B_0 is the strength of the uniform magnetic field, and L is the inside radius of the pipe. This three-dimensional pressure drop is $O(c^{-\frac{1}{3}}L)$ times the pressure gradient for the fully developed flow in the uniform magnetic field.

1. Introduction

The present problem is related to the flow of liquid lithium through a magnetic confinement fusion reactor. In such a reactor, the plasma is confined in a vacuum by a strong magnetic field, which is produced primarily by superconducting magnet coils (Holroyd & Mitchell 1984).

The liquid-lithium feed and return pipes must pass between the superconducting magnet coils. At these points, the flow passes from a region of negligible magnetic field to a region of very strong magnetic field, or vice versa, over a very short length of pipe. In early fusion design studies, these entrance and exit flows were treated by assuming that the flow remains uniform throughout. Maxwell's equations were solved for the electric currents in a solid conductor moving into or out of a magnetic field. Finally the body force due to these currents gave the total pressure drop. This approach is valid for a weak magnetic field because the fluid inertia is so much greater than the electromagnetic force that the inertia carries the flow through the entrance or exit region with no disturbance. However, a fusion reactor has a very strong magnetic field, so that the electromagnetic force is many times larger than the fluid

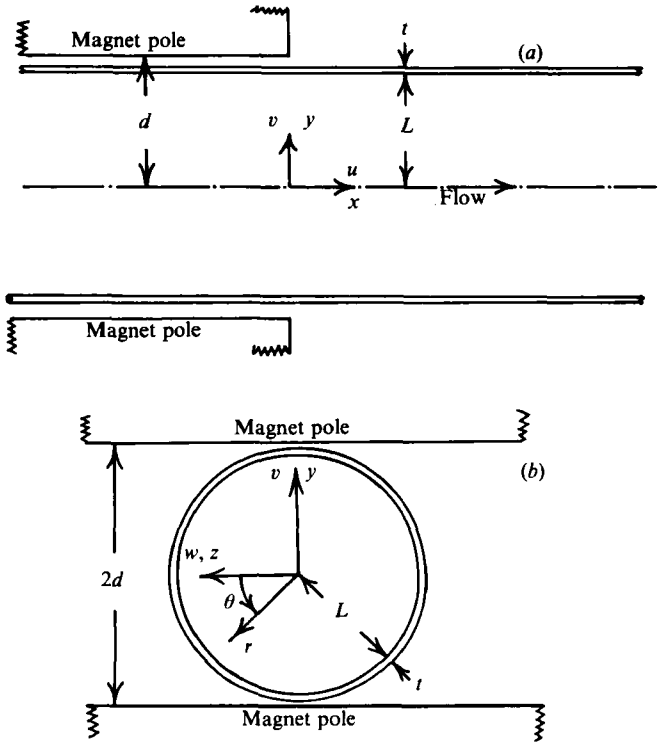

FIGURE 1. Sections of a thin-walled circular pipe and a magnet showing coordinates and velocity components. (*a*) Longitudinal section $z = 0$. (*b*) Cross-section $x = 0$.

inertia. In a feed pipe, the flow deviates radically from uniform flow where the pipe enters or leaves the magnetic field. Therefore, the moving-solid-conductor solution does not apply.

The present paper treats the liquid-metal flow in a straight circular pipe with a thin metal wall. A magnet with parallel poles ends abruptly at $x = 0$, where x is measured along the pipe centreline (see figure 1). The analysis applies for flows both into and out of the magnetic field. The results show that the moving-solid-conductor solution overestimates the pressure drop by at least one order of magnitude. The dimensionless pressure drop from the moving-solid-conductor solution is $O(1)$, while the pressure drop from the present solution is $O(c^{\frac{2}{3}})$, where c is the wall conductance ratio, and $c = 0.01$ is a typical value for a fusion-reactor lithium flow.

The present problem is related to another problem of importance for blanket calculations. If a pipe or duct in a uniform magnetic field has an elbow so that the flow passes between a region with a large transverse magnetic field and a region with a small transverse field, then the flow is similar to that in a straight pipe or duct entering or leaving a magnetic field. The flows are not identical because the large axial magnetic field on one side of the elbow is absent from the entrance–exit problem, and this axial magnetic field affects the flow significantly. However, the flows have many qualitative similarities, and the present analysis will help guide any future analyses of the elbow problem.

2. Basic formulation

The dimensionless equations governing the steady flow of an electrically conducting, incompressible fluid in the presence of a steady magnetic field are

$$N^{-1}(\boldsymbol{v}\cdot\nabla)\boldsymbol{v} = -\nabla p + \boldsymbol{j}\times\boldsymbol{B} + M^{-2}\nabla^2\boldsymbol{v}, \tag{1a}$$

$$\boldsymbol{j} = -\nabla\phi + \boldsymbol{v}\times\boldsymbol{B}, \quad \nabla\cdot\boldsymbol{v} = 0, \tag{1b, c}$$

$$\nabla\cdot\boldsymbol{j} = 0, \quad \nabla\cdot\boldsymbol{B} = 0, \quad \nabla\times\boldsymbol{B} = R_{\mathrm{m}}\boldsymbol{j}, \tag{1d–f}$$

(see e.g. Shercliff 1965 p. 24). Here $\boldsymbol{v}$, p, $\boldsymbol{j}$, $\boldsymbol{B}$ and ϕ are the velocity, pressure, electric current density, magnetic field and electric potential function respectively, which are normalized with respect to V_0, $\sigma V_0 B_0^2 L$, $\sigma V_0 B_0$, B_0 and $V_0 B_0 L$ respectively. Here, V_0, B_0 and L are the characteristic velocity, magnetic field strength and length, while σ is the fluid's electrical conductivity. The dimensionless parameters,

$$N = \frac{\sigma B_0^2 L}{\rho V_0}, \quad M = B_0 L(\sigma/\eta)^{\frac{1}{2}}, \quad R_{\mathrm{m}} = \mu\sigma V_0 L,$$

are the interaction parameter, Hartmann number and magnetic Reynolds number respectively, where ρ, η, and μ are the fluid's density, viscosity and magnetic permeability, which, along with σ, are assumed to be constants. The present analysis concerns the flow in a straight, circular pipe near the end of a long, wide magnet, as shown in figure 1. The inside radius of the pipe is chosen for L, the average axial velocity is chosen for V_0, and the strength of the uniform magnetic field between the poles and far from the ends or sides of the magnet is chosen for B_0.

We assume that $R_{\mathrm{m}} \ll 1$, so that we can neglect the induced magnetic field due to the electric currents in the fluid and pipe wall. It turns out that the largest currents are $O(c^{\frac{2}{3}})$, where $c = \sigma_{\mathrm{w}} t/\sigma L$ is the small wall conductance ratio, while σ_{w} and t are the electrical conductivity and thickness of the pipe wall. Therefore, the neglected induced magnetic field is actually $O(c^{\frac{4}{3}}R_{\mathrm{m}})$. For the flow problem, $\boldsymbol{B}$ is a known vector field, obtained by solving equations (1*e*,*f*) with zero on the right-hand side of (1*f*). We assume (*a*) that the length, width and thickness of the magnet poles are all much larger than the gap, $2d$, and (*b*) that the susceptibility of the poles is large. Then the solution for the plane magnetic field,

$$\boldsymbol{B} = B_x(x,y)\,\hat{\boldsymbol{x}} + B_y(x,y)\,\hat{\boldsymbol{y}},$$

in the central region where the pipe is located, involves a straightforward application of a Schwarz–Christoffel transformation. Walker & Buckmaster (1979) present contours of the magnetic-field strength throughout the non-uniform-field region near and beyond the end of the magnet. The present analysis requires the asymptotic solutions for large x, i.e. far beyond the end of the magnet. These solutions are

$$B_x = -\frac{\beta y}{x^2} + O(x^{-4}), \quad B_y = \frac{\beta}{x} + O(x^{-3}), \tag{2a, b}$$

where $\beta = 2d/\pi L$.

We also assume (*a*) that $M \gg 1$, so that viscous effects are confined to boundary layers, (*b*) that N is sufficiently large that the inertial terms on the left-hand side of (1*a*) are negligible everywhere, and (*c*) that the thin-conducting-wall approximation holds, namely $t \ll L$ and $M^{-1} \ll c \ll 1$. The precise condition on N is determined as

part of the solution. With the thin-conducting-wall approximation, the boundary conditions are

$$j_r = -c\left(\frac{\partial^2\phi}{\partial\theta^2}+\frac{\partial^2\phi}{\partial x^2}\right), \quad v = 0, \quad \text{at } r = 1, \tag{3a, b}$$

where (r, θ, x) are cylindrical coordinates, as shown in figure 1 (*b*) (Holroyd & Walker 1978). With the assumptions that the induced magnetic fields and the inertial effects are negligible, the governing boundary-value problem (1*a–d*), (3), with zero on the left-hand side of (1*a*), is linear. Therefore, the solutions for the flows out or into the magnetic field (flows in the plus or minus x-direction in figure 1*a*, respectively) are identical except for sign differences for certain variables. We need only consider flow out of the magnetic field, i.e. in the plus x-direction in figure 1 (*a*).

For thin-wall pipes or ducts in non-uniform magnetic fields, there are certain characteristic surfaces for the inertialess, inviscid-core solutions, i.e. for the flow outside the viscous boundary layers. The analysis for these characteristic surfaces and an interpretation of their physical significance are given by Holroyd & Walker (1978), and a few of their results are reproduced here. For each magnetic-field line, the integral

$$\zeta = \frac{1}{2}\int_0^{s_0} B^{-1}\,\mathrm{d}s, \tag{4}$$

has a value. Here, s is the distance measured along the magnetic-field line from its first intersection with the inside surface of the pipe or duct to its second intersection at $s = s_0$, while $B(s)$ is the local magnetic field strength at each point on the magnetic-field line. A set of magnetic-field lines inside the fluid with the same value of ζ constitutes a characteristic surface. Neglecting $O(c)$ terms, p must be constant on the characteristic surfaces, while $\boldsymbol{j}$ must be tangent to the surfaces and tangent to the pipe wall at each surface–wall intersection. Similarly, neglecting terms which are comparable to the electric current density component tangent to the characteristic surfaces, ϕ must be constant on the surfaces and $\boldsymbol{v}$ must be tangent to them.

In the uniform magnetic field far upstream of the end of the magnet, $\zeta = (1-z^2)^{\frac{1}{2}}$, and the characteristic surfaces are the planes z = constant. As the flow approaches and passes the end of the magnet, B decreases from 1 to 0, and the characteristic surfaces move away from $z = 0$ and toward $z = \pm 1$ in order to maintain constant ζ. New surfaces for $\zeta > 1$ appear at $z = 0$ and also move toward $z = \pm 1$ downstream. As $x \to \infty$ and $B \to 0$, all characteristic surfaces for finite ζ converge to the points $y = 0$, $z = \pm 1$, as sketched in figure 2. In the uniform field far upstream, the flow is fully developed, and the non-zero core variables are

$$u = 1, \quad \phi = \frac{z}{(1+c)}, \quad j_z = \frac{c}{(1+c)}, \quad \frac{\mathrm{d}p}{\mathrm{d}x} = -\frac{c}{(1+c)}, \tag{5a–d}$$

(Shercliff 1956), where $\boldsymbol{v} = (u, v, w)$. Actually, this solution assumes that $t \ll L$, but treats c as an arbitrary, i.e. $O(1)$, constant, and neglects $O(M^{-1})$ terms. Since we assume that $M^{-1} \ll c \ll 1$, we replace $(1+c)$ by 1 in the solutions (5). It turns out that $j = O(c^{\frac{1}{2}})$ in the non-uniform-field region near the end of the magnet, so that the $O(1)$ flow, which is uniform far upstream, must follow the characteristic surfaces for $0 \leqslant \zeta \leqslant 1$ toward the points $y = 0$, $z = \pm 1$. Since the geometry is symmetric about the plane $z = 0$, the flow is also symmetric and $w = 0$ at $z = 0$. All the characteristic surfaces for $\zeta > 1$ intersect the $(z = 0)$-plane at right angles, so that the tangential velocity along these surfaces is zero here. A characteristic surface is a stream surface for the $O(1)$ velocity, so this velocity is zero on all the surfaces for $\zeta > 1$. The velocity

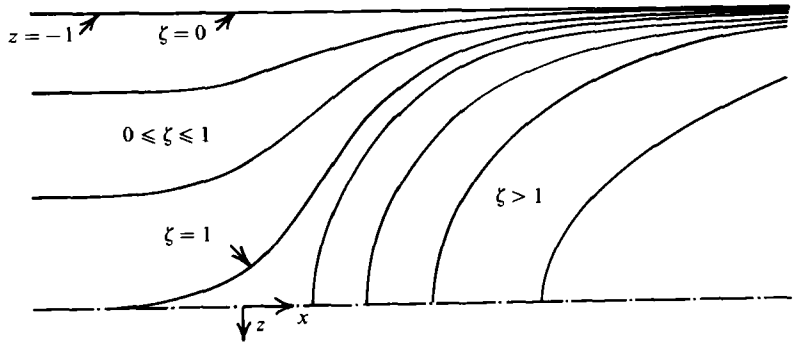

FIGURE 2. Sketch of the intersections of the characteristic surfaces with the $y = 0$ plane for $-1 \leqslant z \leqslant 0$.

in this region is $O(c^{\frac{1}{3}})$. As x increases and B decreases, u near $y = 0$, $z = \pm 1$ becomes large, and the assumptions for the characteristic-surface solution fail. Physically, the magnetic field becomes too weak to hold the flow on the characteristic surfaces, so that the flow begins to migrate across these surfaces and back toward a more uniform flow.

As long as $x = O(1)$, then $B = O(1)$, $\boldsymbol{v} = O(1)$ on the characteristic surfaces for $0 \leqslant \zeta \leqslant 1$, and the characteristic-surface solution is valid. To consider the change in the relationships between the terms in (1) which reverses the evolution toward the high-velocity jets near $y = 0$, $z = \pm 1$, we consider $x = O(\delta^{-1}) \gg 1$, where δ is a small parameter to be determined. Then the solutions (2) indicate that $B_y = O(\delta)$ and $B_x = O(y\delta^2)$. The characteristic surfaces for $0 \leqslant \zeta \leqslant 1$ have become concentrated in the side regions for $(1-\delta^2)^{\frac{1}{2}} = 1 - O(\delta^2) \leqslant |z| \leqslant 1$, as indicated in figure 3. Therefore, for the side regions carrying the $O(1)$ flow, $\partial/\partial x = O(\delta)$, $\partial/\partial y$ and $\partial/\partial\theta$ are $O(\delta^{-1})$, $\partial/\partial z = O(\delta^{-2})$, and $B_x = O(\delta^3)$ because $y = O(\delta)$. Conservation of mass indicates that $u = O(\delta^{-3})$ since the area of the side region is $O(\delta^3)$. If all three scalar terms in the continuity equation (1*c*) are comparable, namely $O(\delta^{-2})$, then $v = O(\delta^{-1})$ and $w = O(1)$. For ϕ, the fully developed-flow solution (5*b*) and the fact that ϕ is constant on the characteristic surfaces (until their assumptions fail) indicate that ϕ is $O(1)$ in the side regions, but varies from 0 to $O(1)$ over an $O(\delta^2)$ transverse distance. This is compatible with the orders of the x- and z-components of $\boldsymbol{v} \times \boldsymbol{B}$ in the Ohm's law (1*b*). Therefore $\partial^2\phi/\partial\theta^2 = O(\delta^{-2})$ at $r = 1$, so that the boundary condition (3*a*) indicates that $j_r = O(c\delta^{-2})$ at $r = 1$. To be valid for the side regions, the boundary condition (3*a*) requires that $t \ll \delta L$. The order of j_r implies that $j_z = O(c\delta^{-2})$ in the side regions. If all three scalar terms in (1*d*) are comparable, namely $O(c\delta^{-4})$, then $j_x = O(c\delta^{-5})$ and $j_y = O(c\delta^{-3})$.

The characteristic-surface solution for ϕ and $\boldsymbol{v}$ follows from the equations (1*b*, *c*), the boundary condition on the inviscid-core solution: $v_r = 0$ at $r = 1$, and the fact that $\boldsymbol{j}$ is negligible in the Ohm's law (1*b*). The characteristic-surface solution fails when at least one component of $\boldsymbol{j}$ is comparable to the terms on the right-hand side of Ohm's law. For the side regions, the ratios of the left-hand sides to the right-hand sides of the x-, y- and z-components of the Ohm's law (1*b*) are $O(\delta^{-6}c)$, $O(\delta^{-2}c)$ and $O(c)$, respectively. Therefore, the characteristic-surface solution fails for $\delta = c^{\frac{1}{4}}$, when j_x is comparable to $\partial\phi/\partial x$ and wB_y. Physically, as the flow becomes concentrated as jets near $y = 0$, $z = \pm 1$, u increases much faster than B_y decreases. Hence, $\partial\phi/\partial z$ must become large in order to balance uB_y in the z-component of Ohm's law. Since ϕ is continuous across the wall–fluid interface, this implies a large gradient of ϕ in the

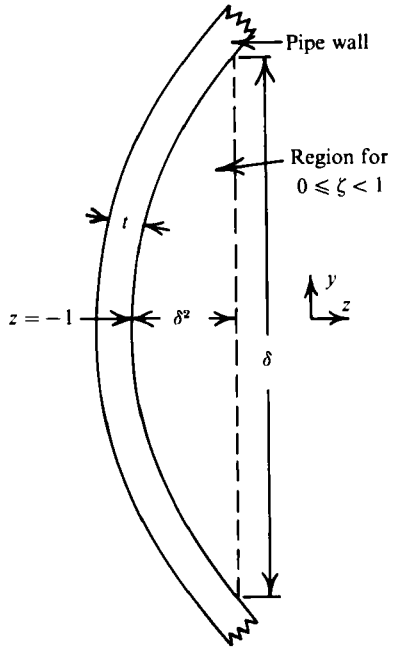

FIGURE 3. Cross-section for $x = O(\delta^{-1}) \gg 1$ showing side region near $y = 0$, $z = -1$ where characteristic surfaces for $0 \leqslant \zeta \leqslant 1$ are concentrated.

pipe wall near $y = 0, z = \pm 1$. This voltage gradient drives electric currents in the wall in the θ direction, and these currents must complete their circuit through the liquid. Part of the wall current entering the liquid turns to flow axially inside the side region. Since this region has a small area, the resultant j_x is large. As B decreases, the flow becomes progressively more concentrated into jets near $y = 0$, $z = \pm 1$, until the j_x from the pipe wall becomes sufficiently large to change the relationships between the terms in the Ohm's law.

An alternate and complementary physical picture is possible. Far upstream $\phi = z$ and far downstream $\phi = 0$, so that there are axial voltage gradients with $\partial\phi/\partial x \lessgtr 0$ for $z \gtrless 0$. These gradients drive axial electric currents in the $\pm x$-directions for $z \gtrless 0$. These currents follow the characteristic surfaces through the core near the end of the magnet and into the side regions downstream. Ultimately the circuit must be completed far upstream and downstream by transverse currents in the pipe wall or in the liquid. In the core near the end of the magnet, the axial currents are spread over an $O(1)$ area, so that j_x is much smaller than $\partial\phi/\partial x$, and Ohm's law dictates that $w \gtrless 0$ for $z \gtrless 0$ in order for $B_y w$ to balance $\partial\phi/\partial x$. Therefore, in the core, the flow must migrate away from $z = 0$ and toward $z = \pm 1$. The characteristic surfaces concentrate the axial currents near $y = 0, z = \pm 1$ as x increases. Eventually, j_x grows to equal and then to exceed $-\partial\phi/\partial x$, so that the sign of w reverses and the flow migrates back toward $z = 0$.

Our first physical 'picture' views the θ variation of ϕ in the pipe wall adjacent to each side region as the important voltage drop; our second physical picture views the overall x-variation of ϕ in the liquid as the important voltage drop. The complete, three-dimensional electric-current circuit involves various subregions of the fluid and adjacent parts of the pipe wall as electrical resistances in series and in parallel. As with any electrical circuit, the current in any part depends on the resistances and

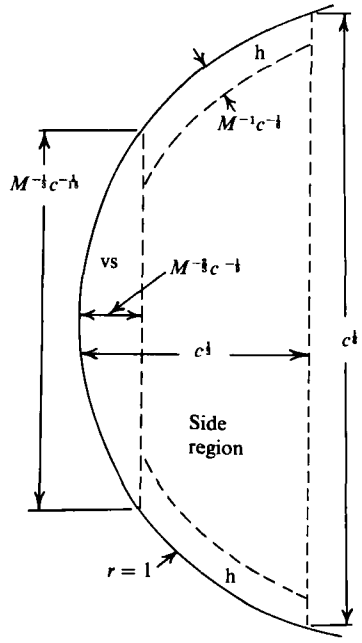

FIGURE 4. The inviscid side region is separated from the wall at $r = 1$ by the Hartmann layers (h) and by the viscous side region (vs).

net electromotive forces in all parts. In §3 we treat the side regions far downstream in the decaying magnetic field. In §4 we treat the upstream completion of the electrical circuit and the resultant perturbation of the fully developed flow. In §5 we attempt an overall picture of the electrical circuit and fluid motion.

3. *Side regions in the decaying magnetic field*

Because of symmetry, we need only consider the side region near $y = 0$, $z = -1$. We introduce

$$x = c^{-\frac{1}{6}}X, \quad y = c^{\frac{1}{6}}Y, \quad z = -1 + c^{\frac{1}{3}}Z, \tag{6}$$

so that the derivatives with respect to the rescaled coordinates, X, Y, Z, are $O(1)$, i.e. are independent of c. For the dependent variables we introduce

$$u = c^{-\frac{1}{2}}U, \quad v = c^{-\frac{1}{6}}V, \quad w = W, \tag{7a–c}$$

$$j_x = c^{\frac{1}{6}}J_x, \quad j_y = c^{\frac{1}{2}}J_y, \quad j_z = c^{\frac{2}{3}}J_z, \tag{7d–f}$$

$$\phi = \Phi, \quad p = c^{\frac{2}{3}}P, \tag{7g, h}$$

where a capital letter denotes the leading term in the asymptotic expansion for a particular side-region variable and is a function of X, Y, Z.

The inertial terms on the left-hand side of the momentum equation (1*a*) are negligible in the side region if

$$N \gg c^{-\frac{5}{3}}.$$

Since this is the most severe restriction on N for any subregion of the flow considered here, it is the assumption required for the present inertialess analysis. The thin-wall approximation, $M^{-1} \ll c \ll 1$, is sufficient to guarantee that the viscous terms in the momentum equation (1*a*) are negligible in the side region. The inviscid side region is separated from the pipe wall by viscous Hartmann layers and a viscous side region, as shown in figure 4. The dimensions of these viscous regions differ from their

traditional dimensions simply because the local magnetic-field strength is $c^{\frac{1}{6}}B_0$, instead of B_0. Therefore, the local Hartmann number $M_L = c^{\frac{1}{6}}M$, the Hartmann layer thickness is $O(M_L^{-1})$ and the viscous side region's dimensions are $O(M_L^{-\frac{2}{3}}) \times O(M_L^{-\frac{1}{3}})$. The Hartmann layers satisfy the boundary conditions (3) and match the side-region variables provided the latter satisfy the condition (3a) and the traditional inviscid velocity condition,

$$v_r = 0, \quad \text{at} \quad r = 1, \tag{8}$$

neglecting $O(M^{-1}c^{-\frac{1}{6}})$ terms. The viscous side region matches the inviscid-side-region variables provided the latter satisfy certain regularity conditions, namely that U and J_x are bounded at $Y = Z = 0$ (Roberts 1967).

We introduce the new independent and dependent variables (6, 7) and the asymptotic form of the magnetic field (2) into the equations (1a–d); we neglect the inertial and viscous terms in the momentum equation (1a); we neglect the terms which are $O(c^{\frac{1}{3}})$ compared to the retained terms; we thus obtain the governing equations for the side region. The variables which satisfy these equations and the symmetry conditions,

$$V = J_y = 0, \quad \text{at} \quad Y = 0,$$

are

$$J_x = \beta^{-1}X\frac{\partial P}{\partial Z}, \quad J_y = -\beta^{-1}Y\frac{\partial P}{\partial Z}, \tag{9a, b}$$

$$J_z = -\beta^{-1}X\frac{\partial P}{\partial X}, \quad U = \beta^{-1}X\frac{\partial \Phi}{\partial Z}, \tag{9c, d}$$

$$V = \beta^{-2}X^2Y\frac{\partial^2 P}{\partial Z^2} - \beta^{-1}Y\frac{\partial \Phi}{\partial Z}, \tag{9e}$$

$$W = -\beta^{-2}X^2\frac{\partial P}{\partial Z} - \beta^{-1}X\frac{\partial \Phi}{\partial X}, \tag{9f}$$

where P and Φ are unknown integration functions of X and Z.

For the side-region variables (6, 7) the boundary conditions (3a, 8) become

$$YJ_y - J_z = -2Z\frac{\partial^2 \Phi}{\partial Z^2} - \frac{\partial \Phi}{\partial Z},$$

$$YV - W = 0, \quad \text{at} \quad Y = \pm(2Z)^{\frac{1}{2}},$$

again neglecting terms which are $O(c^{\frac{1}{3}})$ compared with those retained. We introduce the solutions (9b, c, e, f) into these conditions to obtain the equations governing P and Φ.

$$\beta\left(2Z\frac{\partial^2 \Phi}{\partial Z^2} + \frac{\partial \Phi}{\partial Z}\right) = 2Z\frac{\partial P}{\partial Z} - X\frac{\partial P}{\partial X}, \tag{10a}$$

$$\beta^{-1}X^2\left(2Z\frac{\partial^2 P}{\partial Z^2} + \frac{\partial P}{\partial Z}\right) = 2Z\frac{\partial \Phi}{\partial Z} - X\frac{\partial \Phi}{\partial X}. \tag{10b}$$

For the side region, the integral (4) gives $\zeta = \beta^{-1}X(2Z)^{\frac{1}{2}}$. The equations (10) simplify if we use ζ instead of Z as the transverse coordinate. When we introduce

$$Z = \frac{\beta^2\zeta^2}{2X^2}. \tag{11}$$

The equations (10) become

$$X\frac{\partial^2 \Phi}{\partial \zeta^2} = -\beta \frac{\partial P}{\partial X}, \tag{12a}$$

$$X^3\frac{\partial^2 P}{\partial \zeta^2} = -\beta^3 \frac{\partial \Phi}{\partial X}, \tag{12b}$$

for $0 \leqslant X, \zeta < \infty$. The characteristic surfaces play a key role in the solutions for all subregions. In the core near the end of the magnet, p and ϕ are constant on the characteristic surfaces, i.e. are functions of ζ only. In (12), the right-hand sides represent the variations of P and Φ along the characteristic surfaces $\zeta =$ constant. The left-hand sides show (a) that there are no variations along these surfaces at $X = 0$ where the side region must match the core near the end of the magnet and (b) that the variations along the characteristic surfaces increase with increasing X until P and Φ become uniform across all characteristic surfaces, i.e. until $\partial/\partial\zeta \to 0$.

The regularity conditions that U and J_x are bounded at $Y = Z = 0$ become the boundary conditions

$$\frac{\partial \Phi}{\partial \zeta} = \frac{\partial P}{\partial \zeta} = 0, \quad \text{at} \quad \zeta = 0. \tag{13}$$

For $x = O(c^{-\frac{1}{6}})$, the $O(1)$ flow is concentrated in the side regions, so that the $O(1)\, u = 0$ in the core region between the two side regions in the decaying magnetic field. Since $j_z \ll 1$ here, Ohm's law (1b) and the symmetry condition, $\phi = 0$ at $z = 0$, indicate that the $O(1)\,\phi = 0$ throughout this core. Therefore matching between the side region and the adjacent core gives the boundary conditions

$$\Phi \to 0, \quad P \to \text{constant}, \quad \text{as } \zeta \to \infty, \tag{14}$$

where the second condition follows from (12). The only condition required far downstream is that Φ and P do not grow exponentially as $X \to \infty$.

Some of the $O(c^{\frac{2}{3}})$ total electric current associated with the evolution of the side regions follows the characteristic surfaces into the core near the end of the magnet. For the current on the surfaces for $\zeta > 1$, which close in this core (see figure 2), the electric circuit is completed near the end of the magnet. However, the current on the characteristic surfaces for $0 \leqslant \zeta \leqslant 1$ follows these surfaces into the region of uniform magnetic field. As we shall see in §4, an $O(c^{-\frac{1}{2}})$ length of pipe is required for this current to complete its circuit upstream, and the fully developed flow is disturbed over this pipe length upstream of the end of the magnet. However, we shall also see that the perturbation of the fully developed ϕ is $O(c^{\frac{1}{6}})$, so that the $O(1)\,\phi$ is given by $\phi = z$ throughout the uniform-field region. Since the core near the end of the magnet matches the upstream solution in the uniform magnetic field as $x \to -\infty$ and matches the downstream side-region solution in the decaying magnetic field as $x \to \infty$, since variations of ϕ along the characteristic surfaces in this core are $O(c^{\frac{2}{3}})$, and since v and ϕ are $O(c^{\frac{2}{3}})$ on the surfaces for $\zeta > 1$ in this core, the solution in the side region in the decaying magnetic field must satisfy the boundary condition

$$\Phi = \left\{ \begin{array}{ll} -(1-\zeta^2)^{\frac{1}{2}}, & \text{for } 0 \leqslant \zeta \leqslant 1, \\ 0, & \text{for } 1 < \zeta < \infty, \end{array} \right\} \quad \text{at } X = 0, \tag{15}$$

neglecting $O(c^{\frac{1}{6}})$ terms. The $O(c^{\frac{1}{6}})$ terms neglected in these matchings are the largest terms neglected in the present analysis. Therefore, the first perturbation of the present side-region solution involves terms which are $O(c^{\frac{1}{6}})$ compared to those in (7).

We introduce Fourier cosine transforms,

$$\Phi = 2\pi^{-1}\int_0^\infty \cos(\lambda\zeta)\,\bar{\Phi}(X,\lambda)\,\mathrm{d}\lambda, \tag{16}$$

and a corresponding transform for P. The cosine transforms incorporate the boundary conditions (13) and (14) and reduce (12) to a pair of coupled, homogeneous, first-order ordinary differential equations in X, governing $\bar{\Phi}$ and $\bar{P}$. The transform of the boundary condition (15) gives

$$\bar{\Phi} = -\frac{\pi J_1(\lambda)}{2\lambda}, \quad \text{at} \quad X = 0, \tag{17}$$

where J_1 is the Bessel function of the first kind and first order. The solutions of the transformed equations, which satisfy the boundary condition (17) and which do not grow exponentially as $X \to \infty$, can be expressed either in terms of modified Bessel functions of the second kind and of the one-third and two-thirds orders, or in terms of the Airy function and its derivative. The latter is preferable for ease of numerical evaluation:

$$\bar{\Phi} = (3)^{\frac{1}{3}}\pi\Gamma(\tfrac{1}{3})J_1(\lambda)\,\mathrm{Ai}'\left[\left(\frac{\lambda^2}{2\beta^2}\right)^{\frac{2}{3}}X^2\right]/2\lambda, \tag{18a}$$

$$\bar{P} = \left(\frac{3\beta}{16\lambda}\right)^{\frac{1}{3}}\pi\Gamma(\tfrac{1}{3})J_1(\lambda)\,\mathrm{Ai}\left[\left(\frac{\lambda^2}{2\beta^2}\right)^{\frac{2}{3}}X^2\right]. \tag{18b}$$

The solutions for Φ and P are obtained by introducing (18) into the Fourier inversion formula (16), and then the other side-region variables are given by (9).

Explicit evaluations of the integrals (16) for the solutions (18) do not appear possible, so these integrals were evaluated numerically. A 24 point Gauss quadrature was used for the range $0 \leqslant \lambda \leqslant \lambda_0$, and the positive abscissas of a 20 point Gauss–Hermit quadrature were used for the range $\lambda_0 \leqslant \lambda < \infty$. The latter were chosen because of the exponential behaviour of the Airy function and its derivative for large argument. The constant λ_0 was varied over a wide range of values to ensure that the combined quadrature accurately represents the infinite integrals.

Typical results for U and P are presented in figure 5 for $\beta = 0.898$, which corresponds to a magnet gap of 6 in. ($d = 0.076$ m) and a standard commercial steel tube with $L = 0.054$ m. These values come from the design of an experimental apparatus at Argonne National Laboratory, and the particular values of X for the curves in figure 5 correspond to particular local values of B_y in these future experiments. This apparatus is currently being built and so the experimental results corresponding to the present analytical predictions are not yet available. In figure 5(*a*), the flow near the point $y = 0$, $z = -1$ is still accelerating and the fluid is still moving toward this point. At approximately $X = 1$, the flow migration reverses. In figure 5(*b*), the flow near $y = 0$, $z = -1$ is decelerating and the fluid is migrating back toward $z = 0$. As X increases, significant values of U persist to larger values of Z. The side regions are spreading across the entire cross-section of the pipe and U is approaching a uniform velocity. Figure 5(*c*) shows the very rapid acceleration near $Z = 0$, followed by the more gradual deceleration. For figure 5(*d*), the pressure far downstream is chosen as the pressure datum so that $P \to 0$ as $X \to \infty$. The transverse pressure variation is maximum for small values of X and decreases as X increases. This transverse pressure variation is due to $j_x B_y$ in the z-component of the momentum equation (1*a*), so the transverse pressure gradient reflects the magnitude of j_x for the local B_y. The axial pressure gradient is negative near $Z = 0$, but it is

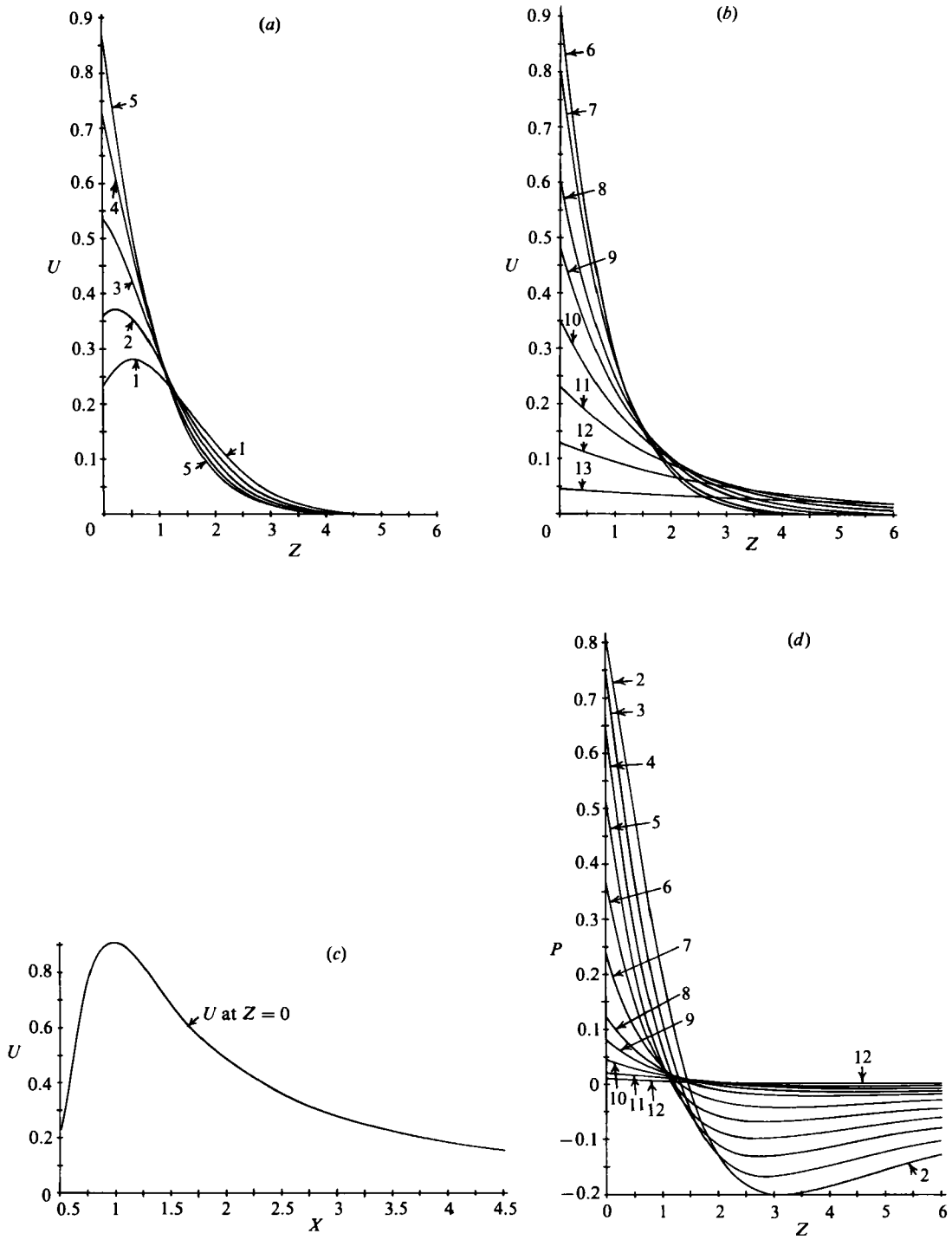

FIGURE 5(*a*)–(*d*). Graphs of axial velocity and pressure in the side region near $z = -1$ in the decaying magnetic field. Here $\beta = 0.898$, $u = c^{-\frac{1}{4}}U$, $p = c^{\frac{3}{4}}P$, $x = c^{-\frac{1}{4}}X$, $z = -1 + c^{\frac{1}{4}}Z$, and $B_y = \beta c^{\frac{1}{4}}/X$. (1) $X = 0.509$; (2) $X = 0.565$; (3) $X = 0.636$; (4) $X = 0.727$; (5) $X = 0.848$; (6) $X = 1.018$; (7) $X = 1.272$; (8) $X = 1.696$; (9) $X = 2.035$; (10) $X = 2.544$; (11) $X = 3.391$; (12) $X = 5.088$; (13) $X = 10.176$.

positive for $Z > 2$. This pressure rise for $Z > 2$ is due to the circulation of electric current in the (y = constant)-planes, frequently called the eddy current due to end effects. In this circulation, $j_z > 0$ upstream in the uniform magnetic field and produces a pressure drop, while $j_z < 0$ downstream in the decaying magnetic field and produces a pressure rise. Since the magnetic field strength is larger upstream, the upstream pressure drop is larger than the downstream pressure rise. The net pressure drop is the pressure loss due to the eddy current. The value of this net pressure drop is determined in the next section.

4. Disturbed fully developed flow in the uniform magnetic field

Holroyd & Walker (1978) treat a problem which differs from the present one only because the magnet poles are doubly infinite in the axial direction and have a step increase in the gap at $x = 0$. The flow passes from a uniform magnetic field with $B_y = 1$ upstream, through a non-uniform magnetic field region near the step in the gap, and into another uniform magnetic field with $B_y = \alpha < 1$, downstream. The flow follows the characteristic surfaces in the core near the step in the gap and enters the downstream weaker uniform magnetic field concentrated as jets in the finite-dimension side regions for $(1-\alpha^2)^{\frac{1}{2}} \leqslant |z| \leqslant 1$. The evolution of these jets near the points $y = 0$, $z = \pm 1$, back across the entire cross-section of the pipe to a uniform flow with $u = 1$ requires an $O(c^{-\frac{1}{2}})$ length of pipe downstream of the step and an $O(c^{\frac{1}{2}})$ circulation of electric current. Part of this current follows the characteristic surfaces through the core near the step and into the upstream stronger uniform magnetic field. An $O(c^{-\frac{1}{2}})$ length of pipe upstream of the step is required to complete the circuit for this current, and the fully developed flow upstream is disturbed over this pipe length. The upstream disturbance is comparable to the fully developed-flow variables, i.e. the disturbance u and ϕ are $O(1)$, and the disturbance pressure is comparable to the $O(c^{\frac{1}{2}})$ pressure drop for fully developed flow over an $O(c^{-\frac{1}{2}})$ length of pipe.

The analysis of Holroyd & Walker (1978) assumes that $\alpha = O(1)$. The present analysis reveals that their solution is valid for $c^{\frac{1}{6}} \ll \alpha < 1$. Flow from a weaker magnetic field to a stronger one is described by their inertialess solution with the flow direction reversed. The present problem corresponds to their problem with $\alpha = 0$. For their problem, the evolution of the jets near $y = 0$, $z = \pm 1$ back to a uniform flow through an $O(1)$ magnetic field requires an $O(c^{\frac{1}{2}})$ electric current circulation; for the present problem, the evolution of the corresponding jets back toward a uniform flow through an $O(c^{\frac{1}{6}})$ magnetic field requires only an $O(c^{\frac{1}{3}})$ electric current circulation. Since the present current disturbing the upstream fully developed flow is $O(c^{\frac{1}{3}})$ instead of $O(c^{\frac{1}{2}})$, all the present upstream disturbance variables are $O(c^{\frac{1}{6}})$ smaller than those for the problem of Holroyd & Walker (1978). The analysis of the upstream perturbation of the fully developed flow in the uniform magnetic field with $B_y = 1$ is very similar to that presented by Holroyd & Walker (1978), so only the key steps and important differences are presented here.

We introduce

$$u = 1 + \beta^{\frac{1}{3}} c^{\frac{1}{6}} u^*, \quad v = \beta^{\frac{1}{3}} c^{\frac{2}{3}} v^*, \tag{19a, b}$$

$$w = \beta^{\frac{1}{3}} c^{\frac{2}{3}} w^*, \quad j_x = \beta^{\frac{1}{3}} c^{\frac{2}{3}} j_x^*, \tag{19c, d}$$

$$j_y = \beta^{\frac{1}{3}} c^{\frac{7}{6}} j_y^*, \quad j_z = c + \beta^{\frac{1}{3}} c^{\frac{7}{6}} j_z^*, \tag{19e, f}$$

$$\phi = z + \beta^{\frac{1}{3}} c^{\frac{1}{6}} \phi^*, \quad p = -c^{\frac{1}{2}} x^* + \beta^{\frac{1}{3}} c^{\frac{2}{3}} p^*, \tag{19g, h}$$

where the starred variables represent the first perturbation of the fully developed flow and are functions of x^*, y, z, while $x^* = c^{\frac{1}{2}}x \leqslant 0$ is the compressed axial coordinate. For the flow in the decaying magnetic field, β is an intrinsic parameter, but for the disturbance to the upstream fully developed flow, β enters only as the multiplicative factor $\beta^{\frac{1}{3}}$ in (19).

We obtain the governing equations by substituting (19) into (1 *a–d*) with $\boldsymbol{B} = \hat{\boldsymbol{y}}$, and by neglecting terms which are $O(c^{\frac{1}{2}}, N^{-1}c^{-\frac{1}{2}}, M^{-2}c^{-1})$ compared with the retained terms. The solutions with $v^* = j_y^* = 0$, at $y = 0$, are

$$j_x^* = \frac{\partial p^*}{\partial z}, \quad j_y^* = 0, \quad j_z^* = -\frac{\partial p^*}{\partial x^*}, \tag{20a–c}$$

$$u^* = \frac{\partial \phi^*}{\partial z}, \quad v^* = y\frac{\partial^2 p^*}{\partial z^2}, \tag{20d, e}$$

$$w^* = -\frac{\partial \phi^*}{\partial x^*} - \frac{\partial p^*}{\partial z}, \tag{20f}$$

where p^* and ϕ^* are unknown integration functions of x^*, z. The boundary conditions (3 *a*, 8) now give the equations governing these two functions

$$(1-z^2)\frac{\partial^2 \phi^*}{\partial z^2} - z\frac{\partial \phi^*}{\partial z} = z\frac{\partial p^*}{\partial x^*}, \tag{21a}$$

$$(1-z^2)\frac{\partial^2 p^*}{\partial z^2} - z\frac{\partial p^*}{\partial z} = z\frac{\partial \phi^*}{\partial x^*}, \tag{21b}$$

for $-\infty < x^* \leqslant 0$, $-1 \leqslant z \leqslant 1$. The regularity conditions from the viscous side regions are that $\partial\phi^*/\partial z$ and $\partial p^*/\partial z$ are bounded at $z = \pm 1$.

We exploit the similarity of the equations (21) and the fact that p^* and ϕ^* are even and odd functions of z respectively. We introduce the eigenfunction expansions

$$\phi^* = \sum_{i=1}^{\infty} a_i[S_i(\theta) - S_i(\pi-\theta)] \exp(\gamma_i x^*), \tag{22a}$$

$$p^* = a_0 + \sum_{i=1}^{\infty} a_i[S_i(\theta) + S_i(\pi-\theta)] \exp(\gamma_i x^*), \tag{22b}$$

into (21) to obtain the ordinary differential equation governing the eigenfunctions

$$\frac{\mathrm{d}^2 S_i}{\mathrm{d}\theta^2} = \gamma_i \cos\theta S_i. \tag{23}$$

for $0 \leqslant \theta \leqslant \pi$. Here $z = \cos\theta$; since p^* and ϕ^* are independent of y, we can solve for them in the plane $y = 0$ with x^*, z or we can solve for them on the lower inside surface of the pipe at $r = 1$, with x^*, θ. The regularity conditions become

$$\frac{\mathrm{d}S_i}{\mathrm{d}\theta} = 0, \quad \text{at } \theta = 0, \pi. \tag{24}$$

The eigenvalue problem (23) and (24), has eigenvalues γ_i which occur in pairs, $\pm\gamma_i$. Since the perturbation of the fully developed flow vanishes as $x^* \to -\infty$, we only want the positive eigenvalues for the solutions (22). Holroyd & Walker (1978) present the first 30 positive values of γ_i. For each value of γ_i, we integrate (23) with a fourth-order Runge–Kutta method and with 2000 steps between 0 and π. Since each S_i behaves

like an Airy function, i.e. exponentially for $0 \leqslant \theta \leqslant \frac{1}{2}\pi$, and sinusoidally for $\frac{1}{2}\pi \leqslant \theta \leqslant \pi$, we normalize each eigenfunction with the initial condition

$$S_i(0) = \exp[-(\tfrac{1}{2}\pi\gamma_i)^{\frac{1}{2}}],$$

so that S_i does not become very large during the integration from 0 to $\frac{1}{2}\pi$.

The coefficients a_i in the expansions (22) are determined by a matching condition at $x^* = 0$. In the problem treated by Holroyd & Walker (1978), the upstream and downstream disturbances of the fully developed flows in different uniform magnetic fields are comparable, and the downstream solution is given by eigenfunction expansions like the expressions (22) with the negative eigenvalues and $x^* > 0$. The upstream and downstream solutions both match the core near the step in the gap where p and ϕ are constant on the characteristic surfaces. These matchings give equalities between p^* and ϕ^* in the upstream and downstream regions, evaluated at $x^* = 0$ and at values of z corresponding to the different positions of a given characteristic surface for the two different magnetic field strengths.

For the present problem, the $O(c^{\frac{1}{3}})$ shift in the order of the upstream disturbance (because of the downstream flow migration across an $O(c^{\frac{1}{6}})$ magnetic field) decouples the upstream and downstream problems. In the previous section, we used the fact that $\phi = z + O(c^{\frac{1}{6}})$ in the upstream uniform magnetic field to derive the boundary condition (15) on the side-region solution in the decaying magnetic field. The $O(c^{\frac{2}{3}})$ pressure in the downstream side region is completely determined by the boundary condition (15). This pressure matches the $O(c^{\frac{2}{3}})$ pressure in the core near the end of the magnet, and this order pressure is constant on the characteristic surfaces in this core. Matching this core and the upstream pressure (19 h) gives

$$\beta^{\frac{1}{3}} p^* = P(0, \zeta), \quad \text{at } x^* = 0, \tag{25}$$

for $0 \leqslant \zeta \leqslant 1$, where $\zeta = (1 - z^2)^{\frac{1}{2}} = \sin\theta$. The variation of $P(0, \zeta)$ for $\zeta > 1$ represents electric current whose circuit is closed within the core near the end of the magnet. The value of $P(0, \zeta)$ is obtained by substituting the solution (18b) with $X = 0$ into the Fourier inversion integral (16). While explicit evaluation does not appear possible, substitution of a standard integral equivalent of J_1 permits explicit integration with respect to λ for $0 \leqslant \zeta \leqslant 1$, to obtain

$$p^*(0, \theta) = (2)^{-\frac{4}{3}}(3)^{\frac{1}{6}}\pi^{-1}\Gamma(\tfrac{1}{3}) \int_{-\frac{1}{2}\pi}^{\frac{1}{2}\pi} \operatorname{sgn}(\Theta - \theta)\, |\sin\Theta - \sin\theta|^{-\frac{2}{3}} \sin\Theta \, \mathrm{d}\Theta. \tag{26}$$

Since the integrand is singular at $\Theta = \theta$, we add and subtract

$$\operatorname{sgn}(\Theta - \theta)\, \sin\theta\, (\cos\theta)^{-\frac{2}{3}} |\Theta - \theta|^{-\frac{2}{3}},$$

to the integrand. The added term is integrated explicitly, and the subtracted term is combined with the original integrand so that there is no singularity at $\Theta = \theta$. In addition, a series solution is necessary near $\theta = \frac{1}{2}\pi$, i.e. $z = 0$, due to the $(\cos\theta)^{-\frac{2}{3}}$ singularity. The values of the integral (26) for 100 values of θ between 0 and $\frac{1}{2}\pi$ are determined using a Simpson's rule method with 200 intervals for $-\frac{1}{2}\pi \leqslant \Theta \leqslant \frac{1}{2}\pi$.

The eigenfunction expansions (22) are truncated after the first 20 positive eigenvalues, and the expansion (22b) is introduced into the boundary condition (26). We choose the coefficients a_i in order to minimize the appropriately weighted integral over $0 \leqslant \theta \leqslant \frac{1}{2}\pi$ of the square of the difference between the left- and right-hand sides of (26). This least mean squared error gives 21 linear algebraic equations for a_0 to a_{20}. The coefficients in these linear equations are integrals of the products of pairs of eigenfunctions, which are not orthogonal, while the inhomogeneous terms are

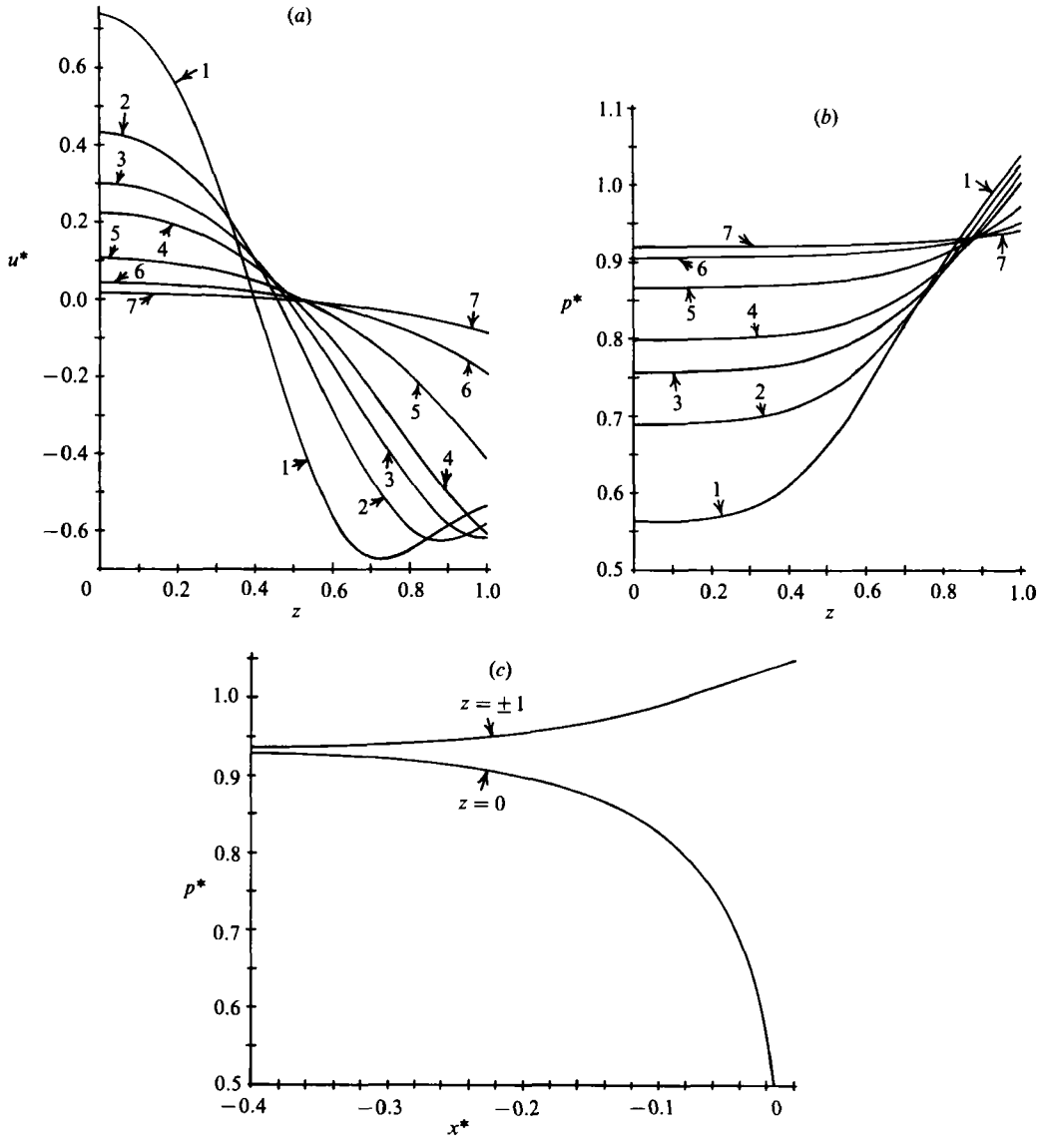

FIGURE 6(*a*)–(*c*). Perturbations of the fully developed flow in the uniform magnetic field. Here $u = 1+\beta^{\frac{1}{3}}c^{\frac{1}{3}}u^*$, $p = -c^{\frac{1}{3}}x^*+\beta^{\frac{1}{3}}c^{\frac{2}{3}}p^*$, $x^* = c^{\frac{1}{3}}x$. (1) $x^* = -0.02$; (2) $x^* = -0.04$; (3) $x^* = -0.06$; (4) $x^* = -0.08$; (5) $x^* = -0.14$; (6) $x^* = -0.22$; (7) $x^* = -0.30$.

integrals of the eigenfunctions times $p^*(0,\theta)$, given by the integral (26). These integrals are evaluated using a Simpson's rule. Once the a_i are determined, the expansions (22) give p^* and ϕ^*, and the equations (20) give the other disturbance variables. We only use 20 eigenvalues because the results are essentially unchanged by increasing the number of eigenvalues further.

The results for u^* and p^* are presented in figure 6. Figure 6(*a*) shows that the flow begins its migration toward the $(z = 0)$-plane before it enters the non-uniform magnetic field. Since this perturbation is ignored by the solution in the decaying magnetic field, we can expect the actual downstream velocity profiles to be slightly less severe than those in figure 5(*a*, *b*), i.e. U near $Z = 0$ should be slightly smaller

and U for large Z should be slightly larger. Figure 6(b) shows that the largest transverse pressure variation occurs near $x^* = 0$ and decreases as $-x^*$ increases. The perturbation pressure increases the axial pressure gradient for $0 \leqslant |z| < 0.8$, and decreases it for $|z| > 0.8$, as shown in figure 6(c). The large pressure drop at $z = 0$ is the pressure drop associated with the eddy current due to end effects.

Far upstream the pressure (19 h) approaches

$$p = -cx + a_0 \beta^{\frac{1}{3}} c^{\frac{2}{3}},$$

where $a_0 = 0.9336$. If we had fully developed flow in a uniform magnetic field with $B_y = 1$, to the end of the magnet, i.e. for $x \leqslant 0$, and fully developed ordinary hydrodynamic (OHD) flow with no magnetic field, beyond the end of the magnet, then the pressure would be given by $p = -cx$, for $x \leqslant 0$, and $p = 0$, for $x \geqslant 0$. We are assuming that the pressure gradient without a magnetic field is negligible. In fact the ratio of the pressure gradients for fully developed OHD and MHD flows in this pipe is $f/2cN$, where f is the traditional friction factor for the OHD flow. Since $N \geqslant c^{-\frac{5}{3}}$, this ratio is much less than $fc^{\frac{2}{3}}$. The difference between the upstream pressures for the actual flow and for the discontinuous fully developed flows is the net pressure drop due to the eddy current, namely,

$$0.9336\, \beta^{\frac{1}{3}} c^{\frac{2}{3}}. \tag{27}$$

The corresponding expression for the problem of Holroyd & Walker (1978) is $kc^{\frac{1}{2}}$, where k depends on α, and $k \to 0$, as $\alpha \to 0$. In (27), the net pressure drop increases as β increases, i.e. as the gradient of the decaying magnetic field decreases. A smaller magnetic-field gradient means that the three-dimensional effects are less severe, but it also means that the magnetic field persists for a longer distance downstream of the end of the magnet. Therefore, the electromagnetic resistance to the flow persists over a longer pipe length and requires a larger overall pressure drop.

5. Concluding remarks

The pressure serves as a stream function for the electric-current density in the fluid. Therefore, the results presented in figures 5(d) and 6(b) (with $-c^{\frac{1}{3}}x^*$ added to the latter) provide a sketch of current lines in the plane $y = 0$, as shown in figure 7. The actual current lines for a given problem would depend on the values of c and β. The axial current lines in the decaying magnetic field are confined to the side regions near $z = \pm 1$ with an $O(c^{\frac{1}{3}})$ transverse dimension, but for most practical values of c, $c^{\frac{1}{3}}$ is not particularly small ($c = 0.01$ gives $c^{\frac{1}{3}} = 0.215$). For the electric currents in the pipe wall, the x-component is everywhere smaller than the θ component, so that each current line leaving the wall at $z = -1$ in figure 7 can be considered to complete its circuit through the wall at that cross-section. Since $\phi \to z$ as $x \to -\infty$ and $\phi \to 0$ as $x \to \infty$, the overall axial voltage variation is linear in z. The axial voltage difference is 0 at $z = 0$ and maximum at $z = \pm 1$. This helps explain why the magnitude of j_x increases with increasing $|z|$. Upstream the wall and liquid represent resistances in series and the e.m.f. is uB_y. The wall has the larger resistance and determines the magnitude of the current, namely $O(c)$. Downstream the wall and liquid represent resistances in parallel and are part of the electrical circuit completed by the axial currents to and from the upstream region and the transverse current in the upstream liquid. The e.m.f.s for this circuit are uB_y at each x and the axial voltage differences.

In the core near the end of the magnet, the electric current follows the characteristic surfaces. Physically the characteristic surfaces arise because the conductor is a liquid

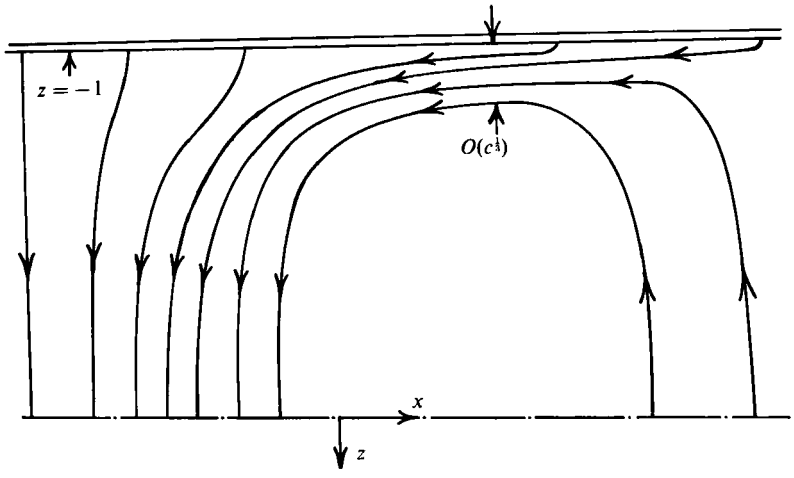

FIGURE 7. Sketch of electric current lines in half of the ($y = 0$)-plane.

instead of a solid. If the liquid were replaced by a moving solid, we would solve the equations (1*b*, *c*) with $\boldsymbol{v} = \hat{\boldsymbol{x}}$ to determine $\boldsymbol{j}$. The momentum equation (1*a*) would be replaced by the equilibrium equation stating that the solid provides whatever stress distribution is needed to balance $\boldsymbol{j} \times \boldsymbol{B}$, up to some strength limit. A liquid in a strong magnetic field has no structure to provide an arbitrary stress field, and this fact is reflected by the momentum equation (1*a*) with $N, M \gg 1$. Only the pressure gradient can balance $\boldsymbol{j} \times \boldsymbol{B}$, so the latter must be irrotational. The current $\boldsymbol{j}$ is still determined by Ohm's law (1*b*), but now $\boldsymbol{v}$ is a variable. If there is a current through the known magnetic field such that $\boldsymbol{j} \times \boldsymbol{B}$ cannot be balanced by ∇p, then the imbalance accelerates the flow until either the inertial or viscous terms re-established equilibrium. This requires a very large $\boldsymbol{v}$, since $N, M \gg 1$. This large $\boldsymbol{v}$ changes the relationship in the Ohm's law (1*b*) until the changing $\boldsymbol{j}$ produces an irrotational body force and $\boldsymbol{v}$ can again become only $O(1)$. In other words, if the current deviates slightly from following the characteristic surfaces, then the flow is accelerated very rapidly and the resultant change in $\boldsymbol{v} \times \boldsymbol{B}$ brings $\boldsymbol{j}$ back to the characteristic surfaces. We would normally think that the momentum equation (1*a*) determines the flow and that the Ohm's law (1*b*) determines the electric current, but, for a liquid metal in a strong magnetic field, these roles are reversed. The electric current is primarily governed by the momentum equation (1*a*) which states what currents the liquid conductor can sustain. Ohm's law (1*b*) then determines the flow distribution whose induced electric field $\boldsymbol{v} \times \boldsymbol{B}$ provides this current.

The flow continues to evolve downstream of the side regions in the decaying magnetic field. The side-region velocity profiles in figure 5(*b*) are spreading across the entire pipe cross-section as $X \to \infty$. We expect the next axial region to have an $O(1)\,u$ throughout and an axial length $\gg c^{-\frac{1}{6}}$. As $B_y \to 0$, the inertialess approximation fails, and we expect inertial effects to be significant in the next axial region. If the Reynolds number, $Re = M^2/N$, is sufficiently large, the flow eventually becomes turbulent, i.e. the local B_y becomes too small to suppress turbulence. We can estimate where this transition will occur for large Re. Transition in a circular pipe with a large Re and with a transverse magnetic field occurs at $N_{\mathrm{cr}} = M_{\mathrm{cr}}/155$ (Branover 1978 p. 156). In the present decaying magnetic field $B_y = \beta/x$, so that the local interaction parameter and Hartmann number are $N\beta^2/x^2$ and $M\beta/x$, respectively. This indicates

transition at approximately $x = 155\,\beta N/M$. Ultimately the flow returns to fully developed OHD pipe flow.

The present analysis ignores the flow evolution beyond the side regions in the decaying magnetic field. The first justification for this is that the pressure variations in this further flow evolution are negligible compared with those treated here. We previously noted that the pressure gradient for an OHD flow is negligible compared to that for the present MHD flow. In the intermediate axial region where inertial and MHD effects are comparable, the pressure gradient is roughly proportional to B_y^2, and B_y^2 is extremely small beyond the side regions. The second justification is that the present analysis captures the essential flow pattern: as the flow enters the non-uniform magnetic field, it becomes concentrated near $y = 0$, $z = \pm 1$, and then, as B_y becomes small, the flow migrates back toward a uniform flow. The inertial and turbulent regions beyond the regions treated here achieve the final adjustment to fully developed OHD flow, but do not affect the basic flow pattern near the end of the magnet.

Holroyd (1980) presents experimental results for a thin-walled circular pipe and a magnet with a step in the poles giving a 50 % reduction in magnetic field strength ($\alpha = 0.5$). However, for the experiments $c = 0.2$, so that $c^{\frac{1}{6}} = 0.765$. The present analysis shows that the analysis of Holroyd & Walker (1978) requires that $\alpha \gg c^{\frac{1}{6}}$, which is clearly not satisfied in Holroyd's experiments. Holroyd finds that the actual dimensionless pressure drop due to the eddy current near the step in the magnet poles is 0.126, while the analysis of Holroyd & Walker gives only 0.073, both relative to two fully developed flows with different B_y and joined at $x = 0$. The present formula (27) gives 0.307 for Holroyd's experiments ($\beta = 0.89$ for $d = 5.0$ cm and $L = 3.58$ cm). The present analysis overestimates the pressure drop for Holroyd's experiments because the analysis has a slow, algebraic decay of B_y to 0, while a step gives a rapid, exponential decay of B_y to 0.5. Nevertheless the result of the present analysis, which corresponds to $\alpha \ll c^{\frac{1}{6}}$, and the result of Holroyd & Walker's analysis, which assumes $\alpha \gg c^{\frac{1}{6}}$, bracket the experimental result for $\alpha = O(c^{\frac{1}{6}})$. The extension of the present analysis to a stepped magnet with $\alpha = O(c^{\frac{1}{6}})$ would be straightforward. In the asymptotic sense, (27) is $O(c^{\frac{2}{3}})$, which is smaller than the corresponding result of Holroyd & Walker, $kc^{\frac{1}{2}}$, where $k = 0.163$ for $\alpha = 0.5$. However, for $c = 0.2$, (27) gives a much larger pressure drop than the result of Holroyd & Walker. While the focus of Holroyd's experiments is the flow near a step in long, parallel pole faces, Holroyd also presents a few pressure measurements near both ends of the magnet. Unfortunately these measurements are only given for roughly two diameters beyond the ends of magnet, and it is not clear what the pressure is approaching in the decaying magnetic field at either end. However, the three-dimensional pressure drops at both ends appear to be the same order of magnitude as the appropriate predictions of the present analysis.

With $c = 0.01$, the assumption that $c \ll 1$ seems reasonable. However, the asymptotic analysis for small c assumes that every positive power of c is also small. The present analysis neglects terms which are $O(c^{\frac{1}{6}})$ compared to the retained terms. Since $c^{\frac{1}{6}} = 0.464$ for $c = 0.01$, the pressure drop prediction (27) and the other results should be viewed as having a possible 50 % error in either direction. The asymptotic analysis predicts that the flow downstream of the end of the magnet is concentrated in the tangent regions near $z = \pm 1$, while the fluid elsewhere is nearly stagnant. However, the transverse dimension of these tangent regions is $O(c^{\frac{1}{3}})$ and $c^{\frac{1}{3}} = 0.215$ for $c = 0.01$. Figure 5 (a) indicates that U approaches 0 at approximately $Z = 4.5$, which corresponds roughly to $z = 0$ for this c. Therefore the velocity profiles in figure 5 (a) actually

just met at the centre of the duct and there is no stagnant region. For the velocity profiles in figure 5(*b*) and for the weaker values of the magnetic field strength U is still significant at $Z = 6.0$, which is beyond the centre of the duct for this c. For these velocity profiles the two tangent regions have spread across the entire duct and are no longer independent as assumed in the asymptotic analysis. What one might expect in an experiment with $c = 0.01$ is that the velocity near $z = 0$ decreases but never actually goes to zero, while the velocity near $z = \pm 1$ increases to perhaps twice the average velocity, corresponding to the peak in figure 5(*c*). In the change of coordinates $X = c^{\frac{1}{6}}x$, x is measured from the end of the magnet. However, since the analysis neglects terms which are $O(c^{\frac{1}{6}})$ compared to those retained, this change of coordinate is actually $X = c^{\frac{1}{6}}(x - x_0)$ where x_0 is an arbitrary position within an $O(1)$ distance of the end of the magnet. This is the reason why the velocity profiles in figure 5 are presented for values of X which correspond to particular values of B_y since in any experiment the position for a particular field strength is known. However, when we plot the pressure as a function of x from the solutions for the disturbance to the fully developed flow, for the flow along characteristic surfaces near the end of the magnet and for the flow migration in the decaying, $O(c^{\frac{1}{6}})$ magnetic field, there is an arbitrariness about where these solutions should be linked, corresponding to the arbitrariness in the origins for X and x^*. As with any asymptotic analysis, the physical point where the inner and outer solutions meet is not defined. The ability of the present asymptotic analysis to predict results for finite values of c can only be confirmed experimentally.

This research was supported by the US Department of Energy through the Fusion Power Program at Argonne National Laboratory under Contract DOE ANL 40952401. The computer programs were executed by Mr Kun-Ho Lie.

REFERENCES

BRANOVER, H. 1978 *Magnetohydrodynamic Flow in Ducts*. John Wiley.

HOLROYD, R. J. 1980 An experimental study of the effects of wall conductivity, non-uniform magnetic fields and variable area ducts on liquid metal flows at high Hartmann number. 2. Ducts with conducting walls. *J. Fluid Mech.* **96**, 355.

HOLROYD, R. J. & MITCHELL, J. T. D. 1984 Liquid lithium as a coolant for Tokamak fusion reactors. *Nuclear Engineering and Design/Fusion* **1**, 17.

HOLROYD, R. J. & WALKER, J. S. 1978 A theoretical study of the effects of wall conductivity, non-uniform magnetic fields and variable-area ducts on liquid-metal flows at high Hartmann number. *J. Fluid Mech.* **84**, 471.

ROBERTS, P. H. 1967 Singularities of Hartmann layers. *Proc. R. Soc. Lond.* A**300**, 94.

SHERCLIFF, J. A. 1956 The flow of conducting fluids in circular pipes under transverse magnetic fields. *J. Fluid Mech.* **1**, 644.

SHERCLIFF, J. A. 1965 *A Textbook of Magnetohydrodynamics*, Pergamon.

WALKER, J. S. & BUCKMASTER, J. D. 1979 Ferrohydrodynamic thrust bearings. *Intl J. Engng Sci.* **17**, 1171.